Cell Death and Differentiation (2004) 11, 1223–1233

www.nature.com/cdd

Expression of apoptosis inhibitor protein Mcl1 linked to neuroprotection in CNS neurons

M Mori[1,3], DL Burgess[1], LA Gefrides[1], PJ Foreman[1], JT Opferman[2], SJ Korsmeyer[2], EA Cavalheiro[3], MdG Naffah-Mazzacoratti[3] and JL Noebels*[,1]

[1] Department of Neurology, Baylor College of Medicine, Houston, TX, USA
[2] Department of Pathology, Dana Farber Cancer Institute, Harvard Medical School, Boston, MA, USA
[3] Universidade Federal de São Paulo – Escola Paulista de Medicina, São Paulo, Brazil
* Corresponding author: JL Noebels, Department of Neurology, Baylor College of Medicine, One Baylor Plaza, Houston, TX 77030, USA. Tel: +1 713 798 5860; Fax: +1 713 798 7528; E-mail: jnoebels@bcm.tmc.edu

Received 19.12.03; revised 21.4.04; accepted 03.5.04; published online 30.7.04
Edited by DW Nicholson

Abstract

Mcl1 is a Bcl2-related antiapoptotic protein originally isolated from human myeloid leukemia cells. Unlike Bcl2, expression has not been reported in CNS neurons. We isolated *Mcl1* in a direct screen for candidate modifier genes of neuronal vulnerability by differential display of mRNAs upregulated following prolonged seizures in two mouse strains with contrasting levels of hippocampal cell death. *Mcl1* is widely expressed in neurons, and transcription is rapidly induced in both strains. In resistant C57Bl/6J mice, Mcl1 protein levels remain persistently elevated in hippocampal pyramidal neurons after seizures, but fall rapidly in C3H/HeJ hippocampus, coinciding with extensive neuronal apoptosis. DNA damage and caspase-mediated cell death were strikingly increased in *Mcl1*-deficient mice when compared to +/+ littermates after similar seizures. We identify *Mcl1* as a neuronal gene responsive to excitotoxic insult in the brain, and link relative levels of *Mcl1* expression to inherited differences in neuronal thresholds for apoptosis.
Cell Death and Differentiation (2004) **11,** 1223–1233.
doi:10.1038/sj.cdd.4401483
Published online 30 July 2004

Keywords: Mcl1; neuronal cell death; seizure; hippocampus; genetics; modifier genes; neuroprotection

Abbreviations: 12 h SE, 12 h after pilocarpine-induced *status epilepticus*; 24 h SE, 24 h after pilocarpine-induced *status epilepticus*; ABC, avidin-biotinylated horseradish peroxidase complex; BH, Bcl2 homology; BH3, Bcl2 domain 3 homology; BSA, bovine serum albumin; C3H, C3H/HeJ; C57, C57Bl/6J; CA3, Ammon's horn subarea 3; CNS, central nervous system; CTX, cortex; DAB, diaminobenzidine dihydrochloride; DbEST, est; DG, dentate gyrus; DTT, dithiothreitol; ECL, enhanced chemiluminescence; ER, endoplasmic reticulum; GAPDH, glyceraldehyde-3-phosphate dehydrogenase; HPC, hippocampus; HPF, high-powered magnification field; IL-6, interleukin-6; JAK, Janus kinase; Klenow, Klenow fragment of DNA polymerase I-mediated biotin-dATP nick-end labeling; MAPK, mitogen-activated protein kinase; Mcl1, myeloid cell leukemia-1; Mcl1-L, myeloid cell leukemia-1 long isoform; Mcl1-S, myeloid cell leukemia-1 short isoform; MEK, mitogen-activated protein kinase kinase kinase; MRNA, messenger RNA; NGS, normal goat serum; Nr, nonredundant; NS, Nissl staining; PAGE, polyacrylamide gel; PBS, phosphate buffer saline; PFA, paraformaldehyde; PILO, pilocarpine; RPA, RNase protection assay; RT, reverse-transcribed; RT-PCR, reverse transcription-polymerase chain reaction; SC, sense control; SDS, sodium dodecyl sulfate; SE, status epilepticus; sm, scopolamine methyl nitrate; SSC, saline-sodium citrate; STAT, signal transducer and activator of transcription; TBS, Tris buffer saline; TdT, terminal deoxynucleotidyltransferase; TGFβ, transforming growth factor beta; TUNEL, terminal deoxynucleotidyl transferase-mediated dUTP end-labeling

Introduction

Neuronal vulnerability to apoptotic death following metabolic stress, ischemia or seizures varies widely among inbred mouse strains, suggesting that this threshold represents a complex genetic trait determined both by genes known to regulate apoptotic pathways as well as modifier loci in the genetic background.[1–6] This relationship has been clearly demonstrated in the brain using targeted mutagenesis. For example, a null mutation has been used to demonstrate that loss of *p53*, a tumor-suppressor gene encoding an executioner protein, protected against seizure-induced hippocampal cell death in hybrid (129/Sv × C57BL/6) mice.[7] However, subsequent genetic dissection indicated that cell loss was extensive when the *p53* null mutation was studied on an inbred 129/Sv genetic strain, implicating a strong contribution from C57BL/6 modifier genes in the earlier study.[8] The identity of these protective modifier genes, which may also be responsible for the differential resistance to cell death observed among other mouse strains, is unknown. Leading candidates include a large number of genes from diverse extracellular and intracellular signaling pathways known to regulate neuronal viability, as well as members of the proteolytic apoptosis cascade itself. Mutations in such genes have also been linked to both proliferative and degenerative cell-specific patterns of human disease affecting the nervous system.[9–11] The characterization of wild-type modifier genes that raise the threshold for cell damage in response to specific types of brain injury could help pinpoint novel molecular targets for therapy based on endogenous mechanisms of neuroprotection.

Two general approaches can be pursued to identify neuroprotective modifier loci *in vivo*. The first utilizes functional information and a candidate gene approach to target the inactivation or overexpression of genes in known apoptotic or antiapoptotic pathways and then to assess the cytopathic effects of altering expression of these genes on different genetic backgrounds. The lack of a complete list of

genes within cell death pathways, the lethality of some null mutants, and the large number of loci and strains that would require extensive analysis make a systematic use of this strategy prohibitive. An alternative approach takes direct advantage of the dramatic differences in cell vulnerability that already exist among various inbred strains of mice. Here we show that the candidate gene approach in mice may be effectively complemented by a reverse genomic strategy that first identifies strain pairs with strong regional differences in neuronal vulnerability, then selects for injury-induced strain-specific differences in gene expression within these regions, and finally evaluates the differentially expressed genes as primary candidates for neuroprotection. This unbiased strategy links variation in transcriptional regulatory cascades to differential cell survival, and in contrast to microarray profiling of pre-selected candidate mRNAs, isolates novel genes as well as known genes within apoptotic pathways that have not yet been localized to brain.

We first determined that C57BL/6J and C3H/HeJ, two commonly studied inbred mouse strains, exhibited clear differences in the degree of cell death following identical episodes of hippocampal seizures. Pilocarpine, a muscarinic cholinergic receptor agonist, is a widely used model of prolonged seizures leading to an early and reproducible pattern of hippocampal cell death.[12] We then used differential display of mRNA transcripts in a genome-wide search to isolate genes that might contribute to this strain-specific vulnerability. Unexpectedly, we identified *Mcl1* as a gene that strongly increased expression in hippocampus following these seizures. Mcl1 is related to the antiapoptotic protein Bcl2, and promotes survival of cultured cells under many conditions that lead to apoptotic cell death.[13–16] Although the founder of this protein family, Bcl2, is considered a crucial regulator of apoptosis in a wide variety of tissues, little attention has been directed toward a role for *Mcl1* in the central nervous system since expression has been reported only in brain epithelial cells and primary CNS tumors, but not in neurons.[17,18] We found that persistence of increased hippocampal Mcl1 protein levels in C57BL/6J, but not in C3H/HeJ brain, correlated with neuroprotection in dentate and pyramidal layer neurons. We used *Mcl1*-deficient mice to confirm the antiapoptotic function of *Mcl1* in brain. Heterozygous *Mcl1* $+/-$ animals had more evidence of DNA damage after seizures than their $+/+$ littermates, demonstrating that *Mcl1* has a significant contribution to the neuronal apoptotic threshold following brain injury.

Results

Strain differences in early apoptotic cell death following seizures

We selected two inbred mouse strains, C57BL/6J and C3H/HeJ, to determine whether genetic differences in thresholds for excitotoxic cell death in the hippocampus could be demonstrated following pilocarpine-induced (PILO) limbic seizures. The acute behavioral features of PILO-induced seizures in C57BL/6J and C3H/HeJ were similar to those reported previously in rats and albino mice.[19] In both strains, PILO treatment induced a stereotyped pattern of behavioral change beginning with akinesia and episodes of forelimb clonus, progressing to recurrent generalized motor seizures that continued as *status epilepticus* (SE). In order to determine whether the effective convulsant dose was strain dependent, PILO was administered (250–400 mg/kg) to both C57BL/6J and C3H/HeJ mice and both seizure severity and survival rates were assessed. At a dose of 250 mg/kg, C57BL/6J showed immobility, followed by brief seizures without progression to prolonged SE, while all C3H/HeJ mice showed SE. At a dose of 350 mg/kg, C57BL/6J mice exhibited SE, while the mortality was high in C3H/HeJ (6/6 mice died immediately following PILO administration). The non-lethal effective doses (250 mg/kg C3H/HeJ, 350 mg/kg C57BL/6J) were selected for subsequent studies. Despite the strain difference in convulsant dose, there were no significant differences regarding seizure progression or duration, and both strains showed SE lasting from 6 to 10 h.

To determine whether an identical interval of SE incurred different degrees of hippocampal cell death between the inbred strains, we performed cresyl violet staining and terminal deoxynucleotidyl transferase-mediated dUTP end-labeling (TUNEL) on mouse brains killed 12 or 24 h after SE onset. Serial sections counterstained for Nissl substance within intact neuronal cell bodies showed disorganization of the pyramidal cell layer in both strains and neuronal cell damage beginning to appear at 12 h after PILO administration; however, few or no cells exhibited positive TUNEL staining and there was no detectable difference in the pattern of cell death in either strain. After a 24 h survival period following SE, Nissl staining revealed a striking increase in shrunken cells with pyknotic nuclei in CA1 and CA3 subareas of C3H/HeJ compared to C57BL/6J mice. Selective TUNEL staining of cell clusters in CA1 and CA3 subareas was clearly evident in both strains; however, despite the lower dose of pilocarpine administered, a greater than three-fold increase in apoptotic cells was found in the pyramidal cell layer of C3H/HeJ compared to C57BL/6J mice (C3H: 104.1 ± 5.2 S.D., $n=7$; C57: 33.5 ± 6.6 S.D.; $n=7$; $P<0.001$; mean number of cells per high-powered field). The highest percentage of apoptotic cells was located within the CA3 region (Figure 1a). C3H/HeJ PILO-treated mice exhibited a small number of TUNEL-labeled cells in DG and other hippocampal regions, but there was no significant difference compared with the same region in C57BL/6J animals (Figure 1b).

Strain comparison of genes regulated by SE

We performed a differential display of mRNA transcripts from hippocampi excised from C57BL/6J and C3H/HeJ mice killed 12 h after PILO-induced SE to screen for potential differences in early gene expression between these strains. Approximately 150 candidate RT-PCR products were identified that were differentially expressed after SE. In all, 10 products showing the most striking differences were eluted from the dried polyacrylamide gels, reamplified by PCR, T/A-cloned, and sequenced. Sequences were then used to query the nonredundant (nr) and est (dbEST) nucleotide divisions of GenBank™ using BLASTN, and the nr protein division using BLASTX. Three of the 10 clones were unambiguously identified; of these, clone 24a showed a high level of

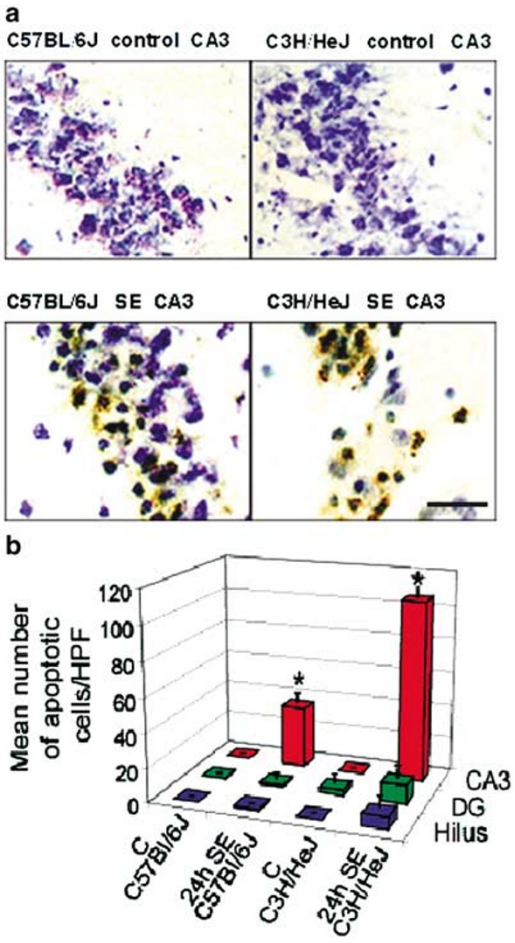

Figure 1 Selective vulnerability to hippocampal cell death in two inbred mouse strains. (**a**) Limbic SE resulted in neuronal damage and TUNEL-positive staining in the hippocampal CA3 region in C57BL/6J and C3H/HeJ mice 24 h after pilocarpine administration. Bar = 50 μm. (**b**) Regional quantification indicates that TUNEL staining is increased greater than three-fold in the CA3 area in C3H/HeJ mice compared with the more resistant C57BL/6J mouse brain. Control: saline control; 24 h SE: pilocarpine-induced SE; HPF: high-powered magnification field; CA3: Ammon's Horn subarea 3; DG: dentate gyrus including hilar polymorphic cell region

sequence similarity to the human *Mcl1* gene (Myeloid Cell Leukemia-1; GenBank BC005427; OMIM 159552) and was selected for further study. *Mcl1* mRNAs for both human (NCBI UniGene Database Cluster Hs.86386) and mouse (NCBI UniGene Cluster Mm.1639) are represented in numerous nervous system tissue samples.

A single Mcl1 spliceform is expressed in adult mouse hippocampus

Two mRNA splice variants of Mcl1 have been described in human tissues; a full-length form (Mcl1-L), which has homology in the C-terminal transmembrane region to Bcl-2 and confers an antiapoptotic function, and a short form (Mcl1-S) with a proapoptotic function.[20,21] To determine which form was being expressed after prolonged seizures, we performed RT-PCR on total RNA extracted from the dissected hippocampi of adult C3H/HeJ and C57BL/6J mice killed 12 h after

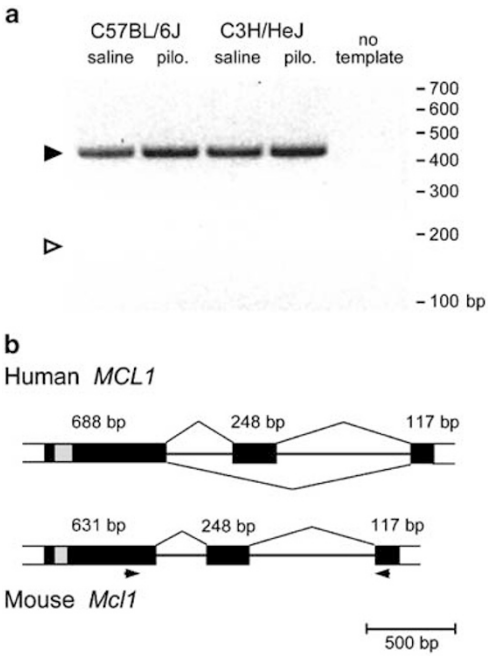

Figure 2 Pilocarpine-induced seizures do not alter Mcl1 mRNA splicing in C57BL/6J or C3H/HeJ mouse brain. (**a**) RT-PCR analysis of RNA extracted from C57BL/6J and C3H/HeJ brains 12 h after injection of saline or seizure-inducing amounts of pilocarpine. A single product was detected in all samples, corresponding to exons 1–3 of Mcl1 (433 bp, black arrowhead). Skipping of exon 2, which generates a proapoptotic form of Mcl1 in some human tissues, was not observed in mouse hippocampus following seizures (185 bp, open arrowhead). (**b**) Comparison of human and mouse Mcl1 gene structures. Mature mRNA transcripts excluding exon 2 are only reported from human tissue. Thick white bars, 5′ and 3′ untranslated regions; thick black bars, coding regions; thin black bars, introns; arrows, primers used for RT-PCR. Diagonal lines indicate confirmed splice patterns. The gray box indicates a region of striking sequence dissimilarity between human and mouse Mcl1. Sizes shown are for coding segments only

either injection of saline or seizure-inducing pilocarpine induced seizures. The products were eluted, purified, and sequenced, and the sequences aligned to human Mcl1-L and Mcl1-S. Mcl1-L, which bears an antiapoptotic function in human cells, was the only form detected in C3H/HeJ or C57BL/6J mouse hippocampus (Figure 2).

In situ hybridization of *Mcl1* in mouse brain

Since Mcl1 expression has not been previously localized in the brain, the distribution of Mcl1 mRNA was determined by *in situ* hybridization to brain sections from untreated C57BL/6J and C3H/HeJ mice. Regional Mcl1 mRNA distribution was diffuse in both strains, and no inter-strain pattern differences were observed (Figure 3a). The strongest labeling pattern was observed in the hippocampal formation, with intense labeling of pyramidal cells in Ammon's horn and granule cells in the dentate gyrus. A strong hybridization signal was also present in neurons in the piriform cortex, entorhinal and perirhinal cortices, amygdala, medial habenula, and the posterior hypothalamic area. Mcl1 mRNA levels were elevated 12 h after an episode of SE. Increased limbic expression following seizures was identified in both strains, and was most prominent in pyramidal and granule cells in the

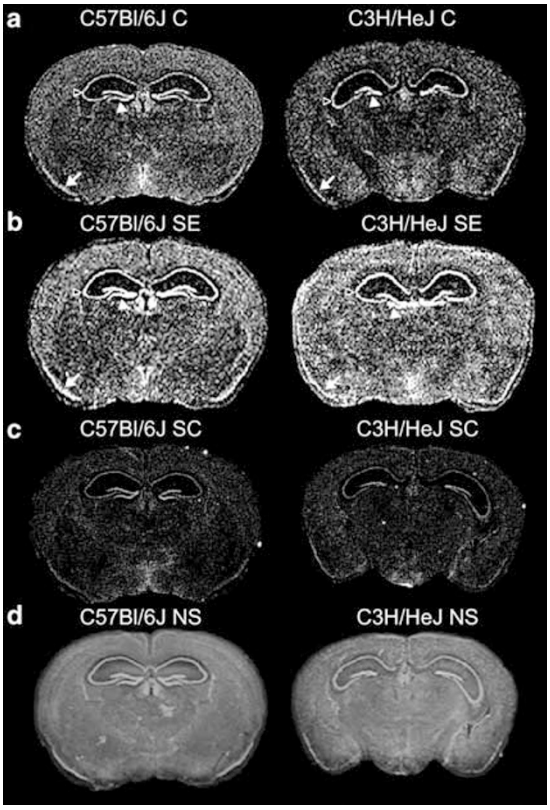

Figure 3 Seizures induce Mcl1 transcription in cell death-resistant (C57BL/6J) and sensitive (C3H/HeJ) mouse strains. *In situ* hybridization of adult mouse brain in (saline-treated animals.) (C) and after pilocarpine-induced SE reveals that Mcl1 mRNA is widely expressed in the brain of both strains, and increases within 12 h following seizures. Seizure-induced Mcl1 expression is most striking in the dentate granule cell and pyramidal cell layers of hippocampus (black and white arrowheads, respectively) as well as in piriform cortex (white arrow). Sense controls (SC) for each strain are shown in third row. The Nissl staining (NS) shows the neuronal cell layers for comparison with corresponding regions in the *in situ* labeling. Photoshop inverted color masking was used in original digital pictures

hippocampal formation, and in the piriform cortices (Figure 3b). There is a very low level of nonspecific binding after probing with the sense probe (Figure 3c). The Nissl staining shows the neuronal areas, which co-localize with the *in situ* labeling for Mcl1 (Figure 3d).

RNase protection assay of Mcl-1

To quantify the altered gene expression found with differential display and *in situ* hybridization, we performed RNase protection assays (RPAs) using Mcl1 riboprobes and hippocampal total RNA extracted 12 h following either saline or SE-inducing PILO injections in both C57BL/6J and C3H/HeJ strains. Three independent RPA experiments were performed. The amount of protected probe was quantified by densitometry of the autoradiographs, and normalized to the housekeeping gene glyceraldehyde-3-phosphate dehydrogenase (GAPDH; GAPDH = 1; Figure 4). Despite an apparent difference based on differential display screening, basal quantitative levels by RPA assay did not statistically differ between strains. However, in both strains, hippocampal Mcl1

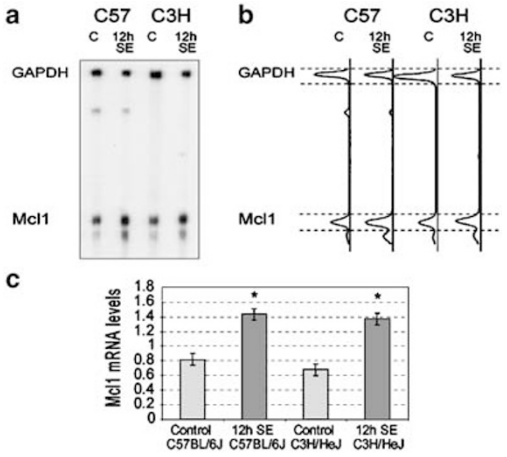

Figure 4 Quantitative ribonuclease protection of Mcl1 mRNA induction by seizures. (**a**) Protection of Mcl1 and GAPDH riboprobes by C57BL/6J (C57) and C3H/HeJ (C3 H) hippocampal RNA extracted 12 h after seizure induction. (**b**) Densitometry profile of the autoradiograph shown in (**a**). Dashed lines demarcate the specific regions quantified. (**c**) Comparison of mean levels of protected riboprobe from three replicate strain-pair comparison experiments, with Mcl1 levels normalized to GAPDH, indicates a significant increase in Mcl1 following seizures in both strains (C). Control; 12 h SE: 12 h after pilocarpine-induced SE

mRNA levels were significantly increased (mean C57BL/6J +76%, range +48 to +133%; mean C3H/HeJ +111%, range +87 to +157%; $P<0.05$) relative to saline-treated control mice of the same strain 12 h after seizures.

Subcellular distribution of Mcl-1 in murine neurons

Immunostaining of limbic regions in mouse brain with anti-Mcl1 antibody showed a diffuse labeling of neurons throughout the neocortex and in pyramidal and dentate granule cell layers within the hippocampal formation. Neurons were clearly labeled by Mcl1 antibody in most layers of the neocortex, although there was preferential staining of larger excitatory cells. In the hippocampal formation, there was strong labeling of dentate granule cells, pyramidal neurons throughout the CA1–4 regions and subiculum, and adjacent entorhinal cortex. We examined the subcellular localization of Mcl1 staining in neurons in mouse brain tissue (Figure 5a). There was a punctate, and occasionally diffuse cytoplasmic pattern sparing the nucleus, generally associated with intense staining near the plasma and nuclear membranes, as described previously in other non-neuronal cell types.[22–24] While staining was most intense in the somatic compartment, immunostaining within large pyramidal neurons was often seen extending away from the soma into the proximal and, rarely, the distal compartments of apical and basilar dendrites.

Diminished Mcl1 immunoreactivity in regions of maximal hippocampal cell loss in C3H/HeJ mice

Limbic seizures increased the intensity of staining in the hippocampus within 12 h in both strains, and at this time point Mcl1 immunoreactivity was greater in the apoptosis-resistant C57 strain (Figure 5b). By 24 h, the maximal intensity staining

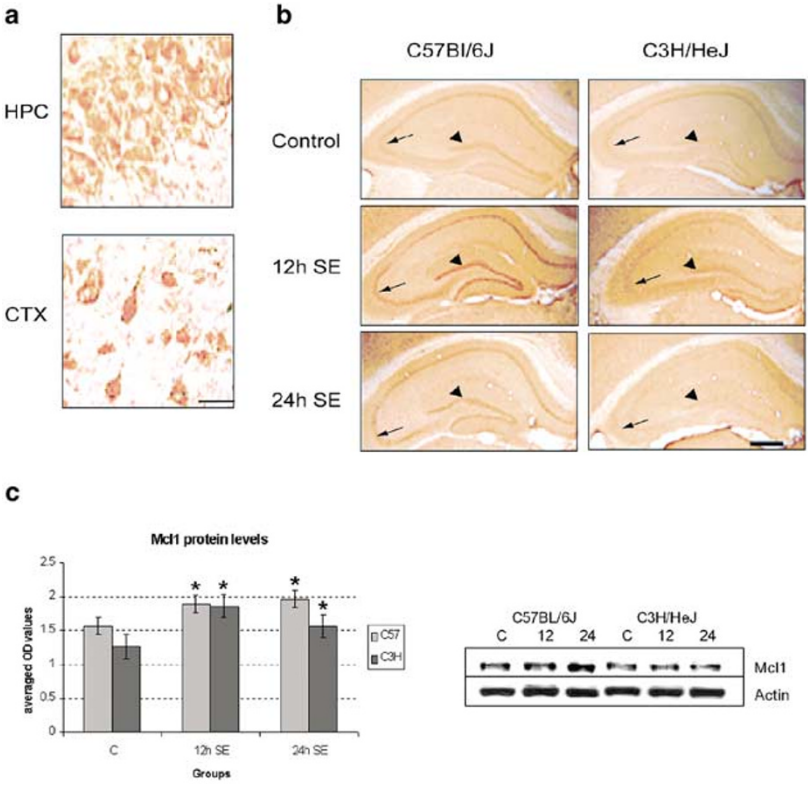

Figure 5 Strain-specific differences in Mcl1 protein following seizures. (**a**) Subcellular localization of Mcl1 in murine neurons. Mcl1 is widely distributed in mouse brain, and shows strong persistent expression in pyramidal cells of (C57BL/6J $+/+$) mouse hippocampus (HPC) and neocortical neurons (CTX) injured by seizure-induced cell death. Mcl1 immunoreactivity shows a perinuclear cytoplasmic localization, extending in larger pyramidal neurons into thicker proximal and apical dendrites. Bar $=50\ \mu$m. (**b**) Decreased level of Mcl1 immunoreactivity in C3H/HeJ hippocampus correlates with increased seizure-induced neuronal apoptosis. Hippocampal sections from cell death-resistant (C57BL/6J) and sensitive (C3H/HeJ) mice before seizures (control animals) show baseline immunostaining levels ($1–2+$), with low to moderate levels apparent in the pyramidal layer (arrow) and dentate granule cell layer (small arrowhead) of both strains. At 12 h after seizure onset (12 h SE), a striking increase ($4+$) in Mcl1 immunoreactivity is evident in C57 pyramidal and dentate cell layers, and lesser ($3+$) increase is observed in C3H. By 24 h (24 h SE), Mcl1 immunostaining in C57 hippocampus remains above pre-seizure levels, but has dropped in C3H to pre-seizure levels. Bar $=400\ \mu$m. (**c**) Histogram showing the results of triplicate Western blotting for Mcl1 protein expression quantifying the differences in the hippocampal protein levels observed by immunohistochemistry, and a representative blot. Blots were probed with anti-Mcl1 and anti-actin as an internal control. There is a significant increase of the Mcl1 protein levels in the period of 12 h after SE in both C3H and C57 strains compared to the control animals (30–47%) ($P<0.05$). At 24 h after SE, Mcl1 protein levels remain significantly elevated in both strains; however, C57 animals were 25% higher than in C3H hippocampi ($P<0.05$), and levels in C3H mice significantly declined by 20%. C: saline control; 12 h SE: 12 h after SE; 24 h SE: 24 h after SE. Bar $=400\ \mu$m

($4+$) in hippocampal fields persisted in C57 brain; however, the same regions in C3H mice showed a clear loss of staining, returning to the moderate baseline intensity ($2+$). This reduction was most striking in regions also showing the most significant levels of cell death, including the hippocampal dentate and pyramidal cell layers. There were no significant changes in the intensity of immunoreactivity evident in other areas of the limbic cortex or related subcortical nuclei. These results were confirmed by Western blotting for Mcl1 that revealed a significant increase (30–47%, $P<0.05$) in the hippocampal protein levels in both strains 12 h after SE. Mcl1 levels remained elevated during the 24 h period following SE in C57 hippocampus, yet decreased during this interval by 25% in C3H animals ($P<0.05$) (Figure 5c).

Mcl1 protects against early apoptotic cell death following SE

To confirm the antiapoptotic function of Mcl1 in neurons as previously shown in other tissues, mice with a targeted deletion of the *Mcl1* gene,[25] (129SvJ/C57BL6 *Mcl1* $-/+$) and $+/+$ littermates, were injected with pilocarpine (350–370 mg/kg) and then compared for differences in the extent of seizure-induced hippocampal cell death. Since homozygous deletion of *Mcl1* results in peri-implantation embryonic lethality, only $+/-$ animals could be used. PILO was administered (300–370 mg/kg) to Mcl1 $+/+$ ($n=15$) and $+/-$ ($n=14$) mice and seizure severity and survival rates were assessed in order to verify whether the lack of one copy of the Mcl1 gene would alter the susceptibility to PILO-induced seizures. At a dose of 350 mg/kg, most wild-type animals showed a single brief seizure consisting of immobility, followed by forelimb and tail extension without progression to SE, while all heterozygotes showed prolonged SE. At a dose of 370 mg/kg, wild-type mice exhibited SE, while the mortality was high (3/3) in heterozygotes. The nonlethal effective doses (350 mg/kg for $+/-$ and 360 mg/kg for $+/+$) were selected for subsequent studies. There were no significant differences regarding seizure progression or duration, and both genotypes showed SE lasting from 6 to 10 h.

To determine whether Mcl1 deficiency alters the threshold for hippocampal cell death after SE, we examined the Klenow fragment of DNA polymerase I-mediated biotin-dATP nick-end labeling (Klenow) for single- and double-stranded DNA breaks, and immunohistochemistry for the activated form of caspase 3. Mcl1-deficient (+/−) and +/+ mice were killed 24 h after SE onset. Minimal Klenow labeling was detected in the hippocampus of saline-treated animals of both genotypes (A, B), whereas there was a striking increase in the number of labeled cells, demonstrating evidence of DNA breaks in the CA3 pyramidal cell layer and other hippocampal subareas of Mcl1 +/− animals when compared to Mcl1 +/+ mice (Figure 6c, d). Activated caspase 3 immunoreactivity was also twice more intense (4+) in Mcl1-deficient mice (F) than wild-type littermates (2+) following seizures (E). The table in Figure 6g shows the three-fold increase in the number of Klenow-labeled cells in animals Mcl1 +/− after seizures compared to their nonaffected littermates (Mcl1 +/+ SE 61±6 S.D., $n=8$; Mcl1 +/− SE: 191±19 S.D.; $n=7$; $P<0.001$; mean number of cells per high powered field; $P<0.001$).

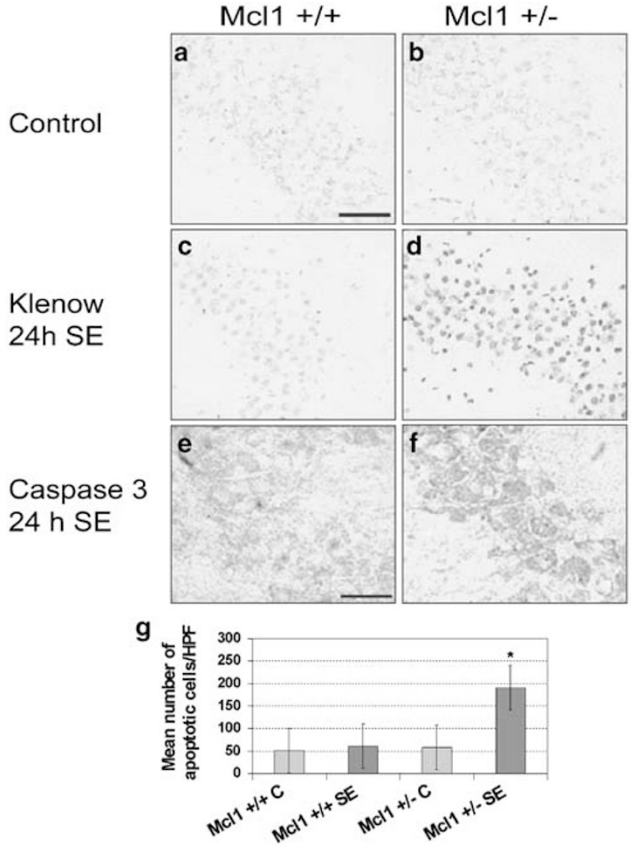

Figure 6 Increased susceptibility to seizure-induced neuronal DNA damage and apoptosis in Mcl1-deficient mice. (**a, b**) No Klenow staining was evident following saline control injections into Mcl1 +/− or +/+ mice. (**c, d**) Prolonged seizures produced DNA damage and Klenow-positive staining in the hippocampal CA3 region in Mcl1 +/− mice 24 h after pilocarpine administration. An intense labeling in neurons within the CA3 pyramidal cell layer is present in +/− mice compared with the Mcl1 +/+ mouse brain after seizures. (**e, f**) Higher immunoreactivity (4+) for caspase 3 was detected in Mcl1 +/− mice 24 h after SE compared to Mcl1 +/+ mouse brain (2+). (**g**) Regional quantification indicates Klenow-labeled cells three times higher in the CA3 area in Mcl1 +/− mice compared with their nonaffected littermates +/+ after seizures ($P<0.001$). Control: saline control; 24 h SE: pilocarpine-induced SE; HPF: high-powered magnification field; CA3: Ammon's Horn subarea 3; Bars denote (**a–d**) 70 μm, (**e, f**) 20 μm

Discussion

We used differential display of hippocampal mRNAs to screen for genes that could contribute to strain-specific differences in vulnerability to apoptotic neuronal cell death following prolonged seizures, and identified Mcl1 expression in brain. Expression of the full-length antiapoptotic Mcl1-L transcript (but not the proapoptotic short form, Mcl1-S) was rapidly upregulated in both sensitive (C3H/HeJ) and resistant (C57BL/6J) strains; however, by 24 h Mcl1 protein levels fell dramatically in the sensitive strain. The sustained presence of Mcl1 protein in surviving cells in the resistant C57 strain, and its rapid decrease in cell layers undergoing apoptosis in the sensitive C3H strain, together with the striking increase in seizure-induced DNA damage within 24 h of a prolonged seizure in Mcl1 +/− mice, provide the first evidence for a protective, inducible role of this protein in neurons in response to brain injury.

Mcl1 belongs to the Bcl2 family of antiapoptotic proteins

Mcl1 is a member of the prosurvival Bcl2 family that constitutes a crucial regulatory point in the mitochondrial pathway leading to apoptosis in a wide variety of tissues. These proteins localize predominantly to mitochondrial membranes, controlling their permeability to cytochrome *c* and Diablo/Smac, and hence downstream activation of the apoptosome complex that initiates a caspase cascade leading to programmed cell death.[26] Antiapoptotic proteins such as the proto-oncogenes Bcl2 and Mcl1 heterodimerize with proapoptotic proteins such as BAD, BOD, Bim, Bik, Bok, and Bax to regulate this death pathway.[27–30] The relative activity of these competing genes, as well as transcription-independent control mechanisms, may determine the apoptotic threshold of the cell. Distribution and expression levels of the individual members are cell, tissue, and differentiation-stage specific, permitting highly selective activation of the cell death program in development and disease.[31–33]

Mcl1 bears significant carboxyl terminus homology (BH1-3 domains) to Bcl-2, and was discovered during a screen for genes that increase expression early in the phorbol ester-induced differentiation of human ML-1 myeloblastic leukemia cells.[13] Mcl1 is located predominantly on mitochondrial outer membranes,[23,24] and promotes survival of cultured cells *in vitro* under many conditions in which cell death occurs due to apoptosis, including growth factor withdrawal, cytotoxic chemical insult, and radiation.[14–16,34] *In vitro* depletion of Mcl1 mRNA and protein by antisense treatment leads to rapid apoptosis of myeloid leukemia cells within 4–18 h,[35,36] and overexpression in hematolymphoid tissues causes disseminated lymphomas of B-cell origin.[37] The relative contribution of Mcl1 is strongly dependent upon cell type; for example,

Mcl1 is the principle antiapoptotic protein in the ovary, while it has a more complex role in other tissues.[16]

MCl1 is active in the apoptotic pathway in CNS neurons

We found diffuse expression of Mcl1 mRNA in mouse brain and a low level of Mcl1 immunoreactivity within murine neurons. Following seizures, the intracellular localization resembles the cytoplasmic staining pattern surrounding the nucleus, mitochondria, and in the endoplasmic reticulum (ER), as seen in lymphoid cells. The intensity of Mcl1 immunoreactivity is known to vary widely among tissues and specific cell types, and is particularly intense in malignant brain neoplasms, including primary central nervous system (CNS) lymphomas and tumors of glial and neuroectodermal origin.[17,18,38] Although those studies found neurons in peripheral dorsal root ganglia that were moderately stained, essentially no neuronal immunoreactivity was reported in the human CNS in these studies. As a result, Mcl1 has remained absent from various lists of candidate genes for cell-death molecules in the nervous system.[31,32,39,40] Since the same antibody to Mcl1 was employed in this study, the disparate immunocytochemical findings are likely explained by the lower antibody titers previously used to examine human neoplastic tissue (1 : 800–1000) compared with the concentration (1 : 200) used in this study, and the fact that neurons were more intensely stained following upregulation by seizures.

Functional link of Mcl1 to neuroprotection in epileptic brain

Several lines of evidence suggest that Mcl1 directly contributes to the neuroprotection observed *in vivo* in C57 mice. First, we found that only the long spliceform of Mcl1 is preferentially expressed in neurons. The human Mcl1 protein has long and short splice variants, with contrasting anti- and proapoptotic properties, respectively.[20,21] The long splice variant produces a prosurvival protein with Bcl2 homology (BH) in domains 1, 2, and 3 and the C-terminal transmembrane region, allowing interactions with diverse Bcl2-related proteins that are lost in the truncated (BH3 only) variant.

Second, activation of Mcl1 begins in the interval preceding the onset of apoptosis. In the initial 12 h following pilocarpine-induced seizures, both the sensitive and resistant inbred strains showed early upregulation of Mcl1 in regions where Klenow-positive DNA breakage, and later TUNEL-positive cell damage, occurs. This early period following seizures coincides with significant upregulation of Bcl2, activation of Fas and FADD death receptor signaling, and caspase-mediated activation of a large number of proteins regulating pro- and antiapoptotic control points in the seizure-induced cell death pathway.[41,42] Mcl1 is upregulated by cytokines such as interleukin-6 (IL6) acting through the JAK/STAT pathway and interferon alpha,[43–46] by activin via the TGFβ pathway[47] and by MEK, implicating the Ras/MEK/MAPK pathway in Mcl1 transcription.[48] Since activity within these linked pathways increases rapidly in CNS ischemia and epilepsy,[49–51] the elevated transcription of Mcl1 may depend on the participation of a wide range of early inflammatory response signaling in the brain. The prompt elevation of Mcl1 expression in both mouse strains after SE suggests that the protein is involved in the earliest response to cell injury, and that upstream regulation is not differentially impaired in the two strains studied.

Third, increased hippocampal Mcl1 immunoreactivity persists in the seizure- and cell death-resistant C57 strain. Elevated levels of Mcl1 protein remained in C57BL/6J hippocampus throughout the 24 h period when apoptotic cell death was initiated, whereas a steep drop in Mcl1 levels coincided with the more extensive pattern of neuronal cell loss in C3 H hippocampus. The Mcl1 protein is highly labile, with a half-life of $\sim$3 h,[23,24] and it is unknown how tightly translation is coupled to steady-state mRNA levels in neurons. These data suggest that a further post-transcriptional step may explain the strain differences in cell vulnerability. Further genetic analyses of these two mouse strains may reveal polymorphisms in Mcl1, in other genes such as the serine/threonine kinase Akt-1 gene,[52] or in various proteases that may account directly for differential Mcl1 protein translation or stability.

Our findings demonstrate that Mcl1 has an important antiapoptotic role in neurons, as demonstrated by the enhanced presence of Klenow labeling of single-stranded DNA breaks in the hippocampus of Mcl1-deficient mice but not $+/+$ mice after SE. Activated caspase-3 immunohistochemistry showed an increased staining intensity in Mcl1-deficient mice 24 h after seizures, indicating that the induction of DNA damage proceeds via caspase-activated deoxyribonuclease. The presence of early Klenow labeling only in Mcl1-deficient mice indicates that Mcl1 acts as an immediate early gene to prevent cell damage in the first 24 h after SE, since single-strand DNA breaks appear to precede double-strand breaks and delayed cell death in other settings.[53,54]

Genomics of neuronal vulnerability in the CNS

We have linked the Mcl1 gene to the increased threshold for seizure induced cell death in C57BL/6J mice compared with C3H/HeJ; however, it is unknown whether this or any single gene accounts for all of the neuroprotection differentiating this strain pair. In addition, while it does not require linkage mapping, the strategy of comparative gene expression profiling isolates only transcriptional differences, and is insensitive to coding polymorphisms altering protein function that might also contribute to variable resistance between the two strains. It is important to emphasize, however, that Mcl1 and the other candidates for regulating differential neuroprotection identified in this study were isolated from what are traditionally considered *wild-type* mouse strains, and not from mice carrying spontaneous or targeted mutations that produce deleterious phenotypes. This strategy therefore helps define the pool of alleles in a general population that are not strictly classified as mutations, but that nonetheless encode a latent susceptibility to tissue injury. Such genes may play an important role in the differential pathological impact of inherited and acquired neurological disorders among individuals. The congruence of induced Mcl1 mRNA and

protein expression with the lowered threshold for damage in Mcl1-deficient mouse brain demonstrates that this member of the Bcl2-related protein family is involved in the apoptotic pathway in central neurons, and may now be included in the list of molecules that modify vulnerability to cell death in both rapid and slow neurodegenerative disease.

Materials and Methods

Seizure induction by pilocarpine

Adult mice (2–3 months of age) of two inbred strains, C57BL/6J and C3H/HeJ, were obtained from breeding colonies of the Jackson Laboratory (Bar Harbor, Maine); Mcl1 $+/-$ and $+/+$ mice were obtained from the colony at Dana Farber Cancer Institute (Boston, MA, USA), and were housed under a 12 h light/dark cycle with *ad libitum* access to food and water. *Status epilepticus* was induced by intraperitoneal injection of pilocarpine hydrochloride (PILO) (Sigma, St. Louis, MO, USA). Scopolamine methyl nitrate (sm) was given 30 min prior to PILO in order to minimize peripheral autonomic effects. Pilocarpine (4%) was dissolved in saline and administered (350 mg/kg i.p. for C57BL/6J; 250 mg/kg for C3H/HeJ; 350 mg/kg Mcl1 $+/-$; 360 for Mcl1 $+/+$) at doses determined by the seizure threshold and mortality rate in these strains to reliably produce seizure episodes lasting 6 h with survival. Control animals, C57BL/6J, C3H/HeJ, Mcl1 $+/-$, and $+/+$ were injected with sm and equal volumes of 0.9% saline instead of PILO.

Apoptosis detection

Groups of C57BL/6J, C3H/HeJ, Mcl1 $+/-$, and $+/+$ mice were decapitated at 12 or 24 h after the onset of behavioral SE. Whole brains were rapidly removed, frozen in isopentane (-40°C), and stored at -80°C. Coronal sections (16 μm thickness) were used for TUNEL, Klenow labeling, and caspase-3 immunohistochemistry.

Detection of DNA strand breaks by TUNEL labeling assay

Sections were formalin fixed at -4°C overnight, washed in 0.1 M phosphate buffer saline (PBS), pH 7.4, post-fixed in pre-chilled ethanol:acetic acid (2 : 1) for 5 min at -20°C. The slices were washed twice in PBS and quenched in 3% H_2O_2, rinsed in PBS and incubated in equilibration buffer for 10 s at room temperature, followed by incubation with terminal deoxynucleotidyltransferase (TdT) (Promega, Madison, WI) in a humid chamber at 37°C for 1 h. Slices were washed in PBS and incubated with anti-digoxigenin peroxidase conjugate at RT for 30 min. Labeling was revealed by application of diaminobenzidine dihydrochloride (DAB). Sections were counterstained with cresyl violet to determine neuronal cell loss.

Detection of DNA strand breaks using Klenow labeling assay

DNA strand breaks were detected on adjacent sections using the Klenow–FragEL kit (Oncogene, San Diego, CA, USA). Briefly, sections were fixed with 4% PFA in PBS for 15 min, washed for 5 min each in TBS, incubated in 2 mg/ml proteinase K in 10 mM Tris (pH 8.0) for 10 min and then washed three times for 5 min each in TBS. After the sections were quenched with 3% H_2O_2 in methanol for 5 min, they were incubated in a humidified air chamber at 37°C for 1 h in the equilibration buffer (0.5 M Tris (pH 8.0), 0.5 M NaCl, 0.1 M $MgCl_2$) for 30 min, followed by incubation in a labeling mixture containing labeled and unlabeled deoxynucleotides and Klenow enzyme for 1.5 h. The reaction was terminated by washing the slides in the stop buffer (0.5 M EDTA, pH 8.0) for 5 min, and then incubated for 5 min in 4% bovine serum albumin in PBS, the slides were incubated with streptavidin/horseradish peroxidase in PBS/bovine serum albumin (BSA) for 30 min at room temperature. The biotin/streptavidin/peroxidase complex was detected by incubating the sections with 0.5 mg/ml DAB in PBS and 0.05% H_2O_2. Sections were dehydrated and coverslipped.

Caspase 3 immunohistochemistry

Adjacent sections were incubated in antigen retrieval solution (Dako, Carpinteria, CA, USA), microwaved for 2 min, incubated for 1 h with 1.5% normal goat serum (NGS) in 0.01 M Tris Buffer Saline (TBS, 100 mM Tris–HCl, 1.5 M NaCl, pH 7.4), then incubated with anti-caspase antibody (1 : 200, Trevigen, Gaithersburg, MD, USA) 1.5% NGS, and 0.25%Triton X-100 overnight at 4°C. After washing in TBS, sections were incubated in biotinylated anti-rabbit antibody (1 μg/ml) diluted in TBS with 1.5% NGS for 30 min, rinsed, and incubated in avidin-biotinylated horseradish peroxidase complex (rabbit ABC staining system, Vecstain, Vector labs, Burlingame, CA, USA) for 30 min. The peroxidase reaction was detected by application of DAB/TBS for 3 min, the sections were rinsed and mounted on slides, dehydrated, cleared, and coverslipped. Regional staining intensity was graded on a 0–4 scale (0 = no visible staining, 4 = intense staining).

Differential display (DD)

Mice were killed 12 h after initiation of SE. Hippocampi from were dissected and immediately frozen on dry ice. TRIzol reagent (Life Technologies) was used to isolate total RNA according to the manufacturer's protocol. To minimize potential DNA contamination, RNA samples were treated with RNase-free DNase I (GenHunter, Nashville, TN, USA). To assess RNA integrity, samples were visualized after electrophoresis through 1.0% agarose gels containing ethidium bromide. Yield and purity were assessed by spectrophotometry. The DD technique was performed using the recommended reagents and manufacturer's protocols supplied with the RNA image kits (GenHunter). Briefly, total RNA isolated from the hippocampus of SE and control animals as described above was reverse-transcribed (RT) in a 20 μl reaction using anchored oligo(dT) primers. In all, 2 μl of the RT reaction was used in PCR with arbitrary 13-mers and anchored oligo(dT) primers in the presence of [α-^{32}P]-dATP according to the methods of Liang *et al*.[55] The products were size-fractionated on 6% denaturing polyacrylamide gels (PAGE) and visualized by autoradiography. The autoradiographs were examined to identify cDNA bands satisfying the following criteria: differential intensity exhibited between PILO-induced C3H/HeJ mice and PILO-induced C57BL/6J mice, when compared to the saline-treated C3H/HeJ and C57BL/6J control mice. These criteria ensured that cDNAs chosen for further analysis would reflect strain-specific alterations due to SE and not those caused by strain variation alone. Bands satisfying these criteria were excised from the dried polyacrylamide gels, and the cDNA eluted, reamplified by PCR, and T/A-cloned into the plasmid vector pGEM-T (Promega) according to the manufacturer's instructions. The resulting clones were sequenced and clone identity was determined using BLASTN alignments to GenBank nr, dbEST, and HTGS database subsets, with default parameters.

Reverse transcription and polymerase chain reaction assay (RT-PCR)

RT-PCR was performed according to the manufacturer's protocol (Access RT-PCR system, Promega). Total RNA was isolated from mouse hippocampus as described above and reverse transcribed (RT) using AMV reverse transcriptase and random hexamers, and the mixtures incubated at 48°C for 45 min followed by 94°C for 2 min. For PCR amplification of Mcl1, the cDNA template resulting from RT of 0.1 μg equivalent of total RNA was used in a 50 μl reaction. The primers were: Mcl1 forward [5′-AGATCATCTCGCGCTACTTGC-3′] and Mcl1 reverse [5′-AGGTCCTGTACGTGGAAGAACTC-3′] (Sigma-Genosys, TX, USA). Amplification consisted of 40 cycles (94°C for 30 s, 60°C for 1 min, 68°C for 2 min), followed by incubation at 68°C for 7 min. In all, 5 μl of loading dye was added to 15 μl of sample, electrophoresed through a 1% agarose gel containing ethidium bromide, and visualized by UV illumination. There are two isoforms for Mcl1, a long form constituted by 433 base pairs and a short form of 185 base pairs, only the long form was detected by the RT-PCR. The bands were eluted, purified from the gel (Qiagen, Chatsworth, CA, USA) and the cDNAs sequenced for authentication.

In situ hybridization

Oligonucleotide probes were constructed from sequenced clones. *In situ* hybridization was performed as outlined by Burgess *et al*.[56] A 45-mer antisense oligonucleotide probe was designed to nonconserved regions of the mouse Mcl1 cDNA [5′-CCTAACCCTTTCGGGAACAGCTGT-TAAAGTGTTAGGTGCTCTACC-3′] (Sigma-Genosys, TX, USA). Probes were 3′ end-labeled using TdT (Promega) and deoxyadenosine 5′-[α-^{35}S]thiotriphosphate (1250 Ci/mmol; NEN) to a specific activity of 10^9 dpm/mg. Unincorporated oligonucleotides were removed using Bio-spin 6 chromatography columns (Bio-Rad, Hercules, CA, USA) and dithiothreitol (DTT) was added to a final concentration of 20 mM. C3H/HeJ and C57BL/6J mice were killed by cervical dislocation 12 h after the onset of SE and 12 μM brain sections from these and sex/age/strain-matched controls were cut in a cryostat and thaw-mounted onto Superfrost/Plus glass slides (Fisher). Sections were fixed in 4% paraformaldehyde (PFA) in PBS, rinsed in PBS and dehydrated in an ascending ethanol series. The hybridization solution contained 50% (v : v) formamide, 4 $\times$ saline-sodium citrate (SSC), 25 mM sodium phosphate, 1 mM sodium pyrophosphate, 10% dextran sulfate (w : v), 5 $\times$ Denhart's solution, 200 μg/ml sonicated (100–600 bps) herring sperm DNA (Promega), 100 μg/ml polyadenylic acid [5′] (Sigma Aldrich, St. Louis, MO, USA), and 5×10^2 dpm of deoxyadenosine 5′-[α-^{35}S]thiotriphosphate-labeled oligonucleotide probe. Nonspecific hybridization was assessed by hybridization of selected sections in the presence of an additional 100-fold unlabeled oligonucleotide. Sections were hybridized under Parafilm coverslips overnight at 42°C, prior to washing in 1 $\times$ SSC at room temperature for 20 min, 0.3 $\times$ SSC at 55°C for 4 min, and 2 $\times$ SSC at room temperature for 5 min. All washing solutions contained 10 mM DTT. Sections were dehydrated in an ascending ethanol series and exposed to Kodak (Rochester, NY) BioMax MR film for 2–5 days. Developed autoradiographs were digitized (Sprintscan 35, Polaroid, Cambridge, MA, USA) and arranged using Photoshop 5.0 (Adobe systems, San Jose, CA, USA).

Ribonuclease protection assay

RPA was utilized to confirm and quantify differences in gene expression obtained by DD. Total RNA preparations from homogenized mice hippocampi were hybridized with cRNA probes followed by digestion with RNAse using protocols and reagents supplied in the RNAse Protection kit (Ambion). Briefly, 5 μg of total RNA was co-precipitated with 1–3 $\times$ 10^5 cpm [^{32}P]-UTP-labeled *in vitro*-transcribed mouse Mcl1 cRNA, then dissolved in 20 μl hybridization buffer. The housekeeping gene GAPDH cRNA was used for normalization. Reaction mixtures were heated to 95°C for 5 min and incubated overnight at 45°C. A mixture of RNaseA/T1 was then added to digest single-stranded RNA, while the cRNA fragments hybridized to the endogenous sense mRNA and were protected from RNAse digestion. The protected cRNA fragments were precipitated with isopropanol and the pellets resuspended in 5 μl gel loading buffer, denatured at 95°C, and fractionated by 6% PAGE. The gel was fixed, dried, and analyzed by autoradiography. Bands representing protected fragments were digitally quantified using Scion-Image/NIH image software.

Reverse transcription and polymerase chain reaction assay (RT-PCR)

RT-PCR was performed according to the manufacturer's protocol (Access RT-PCR system, Promega). Total RNA was isolated from mouse hippocampus as described above and reverse transcribed (RT) using AMV reverse transcriptase and random hexamers, and the mixtures incubated at 48°C for 45 min followed by 94°C for 2 min. For PCR amplification of Mcl1, the cDNA template resulting from RT of 0.1 μg equivalent of total RNA was used in a 50 μl reaction. The primers were: Mcl1 forward [5′-AGATCATCTCGCGCTACTTGC-3′] and Mcl1 reverse [5′-AGGTCCTGTACGTGGAAGAACTC-3′] (Sigma-Genosys, TX, USA). Amplification consisted of 40 cycles (94°C for 30 s, 60°C for 1 min, 68°C for 2 min), followed by incubation at 68°C for 7 min. In all, 5 μl of loading dye was added to 15 μl of the sample, electrophoresed through a 1% agarose gel containing ethidium bromide, and visualized by UV illumination. There are two isoforms of Mcl1, a long form constituted of 433 base pairs and a short form of 185 base pairs, and only the long form was detected in the agarose gel. The bands were eluted, purified from the gel (Qiagen, Chatsworth, CA, USA) and the cDNAs sequenced for authentication.

Mcl1 immunohistochemistry

Mice were anesthetized (i.p.) with ketamine, xylazine, and acepromazine (0.5–1 mg/kg), and perfused transcardially with 0.1 M PBS (pH 7.4), followed by 4% PFA in 0.1 M PBS (pH 7.4). Brains were removed, post-fixed overnight in 4% PFA, transferred to 30% sucrose/PBS, and stored at 4°C. Coronal sections (40 μm thick) were cut in a cryostat at -20°C, and stored in Tris-buffered saline (0.1 M Tris–HCl; 0.15 M NaCl; pH 7.4) (TBS) at 4°C. Floating sections were incubated for 1 h with 1.5% normal goat serum (NGS) in TBS, then incubated with anti-Mcl1 antibody (1 : 200, S-19, Santa Cruz Tech., Santa Cruz, CA, USA), 1.5% NGS, and 0.25% Triton X-100 overnight at 4°C. The Santa Cruz Mcl1 antiserum was obtained using the same sequence as that reported previously and evaluated for specificity.[31,32] After washing in TBS, sections were incubated in biotinylated anti-rabbit antibody (1 μg/ml) diluted in TBS with 1.5% NGS for 30 min, followed by three rinses in TBS for 5 min. Sections were incubated in avidin-biotinylated horseradish peroxidase complex (rabbit ABC staining system, sc-2018, Santa Cruz Tech.) for 30 min and rinsed with TBS. The peroxidase reaction was detected by application of DAB/TBS for 3 min. After rinsing in TBS, sections were mounted on slides, dehydrated, cleared, and coverslipped. Regional staining intensity was

graded on a scale of 0–4 scale (0 = no visible staining, 4 = intense staining).

Western blotting

C57BL/6J and C3H/HeJ mice were killed at 12 and 24 h after pilocarpine-induced SE, and the hippocampi were dissected. The tissues were homogenized in lysis buffer containing 150 nM NaCl, 50 mM Tris–HCl, pH 8.0, 0.1% SDS, 1 mM DTT, 1 mM phenylmethylsulfonyl fluoride, and 50 μl/g tissue of protease inhibitor cocktail (104 mM AEBSF, 0.08 mM aprotinin, 2 mM leupeptin, 4 mM bestatin, 1.5 mM pepstatin A, 1.4 mM E-64, Sigma P 8340, St. Louis, MO, USA). In all, 50 μg of protein (as determined by standard BCA, Pierce, Rockford, IL, USA protein assay) in Laemmli buffer was resolved on SDS–PAGE, followed by electroblotting onto polyvinylidene difluoride membrane. After blocking with blocking solution (Amersham, Little Chalfont, Buckinghamshire, UK) in Tris-buffered saline with Tween 20 (150 mM NaCl, 50 mM Tris–HCl, pH 8.0, and 0.05% Tween 20), the membranes were probed with Mcl1 antibody (1 : 1000, S-19, Santa Cruz Tech., Santa Cruz, CA, USA). After binding with horseradish peroxidase-conjugated secondary antibodies, blots were visualized with an enhanced chemiluminescence (ECL) detection system (Amersham Biosciences). The membrane was analyzed by autoradiography. Mcl1 protein levels were digitally quantified using Scion-Image/NIH image software.

Acknowledgements

This work was supported by NIH 29709 (JLN) and FAPESP, EFA and MFF (MM).

References

1. Xiang H, Kinoshita Y, Knudson CM, Korsmeyer SJ, Schwartzkroin PA and Morrison RS (1998) Bax involvement in p53-mediated neuronal cell death. J. Neurosci. 18: 1363–1373
2. Faherty CJ, Xanthoudakis S and Smeyne RJ (1999) Caspase-3-dependent neuronal death in the hippocampus following kainic acid treatment Brain. Res. Mol. Brain Res. 70: 159–163
3. Holcik M, Thompson CS, Yaraghi Z, Lefebvre CA, MacKenzie AE and Korneluk RG (2000) The hippocampal neurons of neuronal apoptosis inhibitory protein 1 (NAIP1)-deleted mice display increased vulnerability to kainic acid-induced injury. Proc. Natl. Acad. Sci. USA 97: 2286–2290
4. Viswanath V, Wu Z, Fonck C, Wei Q, Boonplueang R and Andersen JK (2000) Transgenic mice neuronally expressing baculoviral p35 are resistant to diverse types of induced apoptosis, including seizure-associated neurodegeneration. Proc. Natl. Acad. Sci. USA 97: 2270–2275
5. Korhonen L, Belluardo N and Lindholm D (2001) Regulation of X-chromosome-linked inhibitor of apoptosis protein in kainic acid-induced neuronal death in the rat hippocampus. Mol. Cell. Neurosci. 17: 364–372
6. Shuttleworth CWR and Connor JA (2001) Strain-dependent differences in calcium signaling predict excitotoxicity in murine hippocampal neurons. J. Neurosci. 21: 4225–4236
7. Morrison RS, Wenzel HJ, Kinoshita Y, Robbins CA, Donehower LA and Schwartzkroin PA (1996) Loss of the p53 tumor suppressor gene protects neurons from kainate-induced cell death. J. Neurosci. 16: 1337–1345
8. Schauwecker PE and Steward O (1997) Genetic determinants of susceptibility to excitotoxic cell death: implications for gene targeting approaches. Proc. Natl. Acad. Sci. USA 94: 4103–4108
9. Roy N, Mahadevan MS, McLean M, Shutler G, Yaraghi Z, Farahani R, Baird S, Besner-Johnston A, Lefebvre C, Kang X, Salih M, Aubry H, Tamay K, Guan X, Ioannou P, Crawford TO, de Jong PJ, Suhr L, Ikeda J-E, Korneluk RG and MacKenzie A (1995) The gene for neuronal apoptosis inhibitory protein is partially deleted in individuals with spinal muscular atrophy. Cell 80: 167–178
10. Li H and Yuan J (1999) Deciphering the pathways of life and death. Curr. Opin. Cell Biol. 11: 261–266
11. Mullauer L, Gruber P, Sebinger D, Buch J, Wohlfart S and Chott A (2001) Mutations in apoptosis genes: a pathogenetic factor for human disease. Mutat. Res. 488: 211–231
12. Turski WA, Cavalheiro EA, Bortolotto ZA, Mello LM, Schwarz M and Turski L (1984) Seizures produced by pilocarpine in mice: a behavioral, electroencephalographic and morphological analysis. Brain Res. 321: 237–253
13. Kozopas KM, Yang T, Buchan HL, Zhou P and Craig RW (1993) Mcl1, a gene expressed in programmed myeloid cell differentiation has sequence similarity to BCL-2. Proc. Natl. Acad. Sci. USA 90: 3516–3520
14. Hockenbery D, Nunez G, Minniman C, Schreiber RD and Korsmeyer SJ (1990) Bcl-2 is an inner mitochondrial membrane protein that blocks programmed cell death. Nature 348: 334–336
15. Garcia I, Martinou I, Tsujimoto Y and Martinou J (1992) Prevention of programmed cell death of sympathetic neurons by the bcl-2 proto-oncogene. Science 258: 302–304
16. Hsu SY and Hsueh AJ (2000) Tissue-specific Bcl-2 protein partners in apoptosis: an ovarian paradigm. Physiol. Rev. 80: 593–614
17. Krajewski S, Bodrug S, Krajewska M, Shabaik A, Gascoyne R, Berean K and Reed JC (1995) Immunohistochemical analysis of Mcl-1 protein in human tissues. Differential regulation of Mcl-1 and Bcl-2 protein production suggests a unique role for Mcl-1 in control of programmed cell death *in vivo*. Am. J. Pathol. 146: 1309–1319
18. Krajewski S, Krajewska M, Ehrmann J, Sikorska M, Lach B, Chatten J and Reed JC (1997) Immunohistochemical analysis of Bcl-2, Bcl-X, Mcl-1, and Bax in tumors of central and peripheral nervous system origin. Am. J. Pathol. 150: 805–814
19. Cavalheiro EA, Santos NF and Priel MR (1996) The pilocarpine model of epilepsy in mice. Epilepsia 37: 1015–1019
20. Bae J, Leo CP, Hsu SY and Hsueh AJ (2000) MCL-1S, a splicing variant of the antiapoptotic BCL-2 family member MCL-1, encodes a proapoptotic protein possessing only the BH3 domain. J. Biol. Chem. 275: 25255–25261
21. Bingle CD, Craig RW, Swales BM, Singleton V, Zhou P and Whyte MK (2000) Exon skipping in Mcl-1 results in a bcl-2 homology domain 3 only gene product that promotes cell death. J. Biol. Chem. 275: 22136–22146
22. Krajewski S, Bodrug S, Gascoyne R, Berean K, Krajewska M and Reed JC (1994) Immunohistochemical analysis of Mcl-1 and Bcl-2 proteins in normal and neoplastic lymph nodes. Am. J. Pathol. 145: 515–525
23. Yang T, Kozopas KM and Craig RW (1995) The intracellular distribution and pattern of expression of Mcl-1 overlap with but are not identical to, those of Bcl-2. J. Cell Biol. 28: 1173–1184
24. Akgul C, Moulding DA, White MR and Edwards SW (2000) *In vivo* localization and stability of human Mcl-1 using green fluorescent protein (GFP) fusion proteins. FEBS Lett. 478: 72–76
25. Rinkenberger JL, Horning S, Klocke B, Roth K and Korsmeyer SJ (2000) Mcl-1 deficiency results in peri-implantation embryonic lethality. Genes Dev. 14: 23–27
26. Gross A, McDonnell JM and Korsmeyer SJ (1999) BCL-2 family members and the mitochondria in apoptosis. Genes Dev. 13: 1899–1911
27. Huang DC and Strasser A (2000) BH3-only proteins – essential initiators of apoptotic cell death. Cell 103: 839–842
28. Bae J, Hsu SY, Leo CP, Zell K and Hsueh AJ (2001) Underphosphorylated BAD interacts with diverse antiapoptotic Bcl-2 family proteins to regulate apoptosis. Apoptosis 6: 319–330
29. Putcha GV, Moulder KL, Golden JP, Bouillet P, Adams JA, Strasser A and Johnson EM (2001) Induction of BIM, a proapoptotic BH3-only BCL-2 family member, is critical for neuronal apoptosis. Neuron 29: 615–628
30. Whitfield J, Neame SJ, Paquet L, Bernard O and Ham J (2001) Dominant-negative c-Jun promotes neuronal survival by reducing BIM expression and inhibiting mitochondrial cytochrome *c* release. Neuron 29: 629–643
31. Merry DE and Korsmeyer SJ (1997) Bcl-2 gene family in the nervous system. Annu. Rev. Neurosci. 20: 245–267
32. Yuan J and Yankner BA (2000) Apoptosis in the nervous system. Nature 407: 802–809
33. Oppenheim RW, Flavell RA, Vinsant S, Prevette D, Kuan CY and Rakic P (2001) Programmed cell death of developing mammalian neurons after genetic deletion of caspases. J. Neurosci. 21: 4752–4760

34. Nijhawan D, Fang M, Traer E, Zhong Q, Gao W, Du F and Wang X (2003) Elimination of Mcl-1 is required for the initiation of apoptosis following ultraviolet irradiation. Genes Dev. 17: 1475–1486
35. Moulding DA, Giles RV, Spiller DG, White MR, Tidd DM and Edwards SW (2000) Apoptosis is rapidly triggered by antisense depletion of MCL-1 in differentiating U937 cells. Blood 96: 1756–1763
36. Derenne S, Monia B, Dean NM, Taylor JK, Rapp MJ, Harousseau JL, Bataille R and Amiot M (2002) Antisense strategy shows that Mcl-1 rather than Bcl-2 or Bcl-x(L) is an essential survival protein of human myeloma cells. Blood 100: 194–199
37. Zhou P, Levy NB, Xie H, Qian L, Lee CY, Gascoyne RD and Craig RW (2001) Mcl1 transgenic mice exhibit a high incidence of B-cell lymphoma manifested as a spectrum of histologic subtypes. Blood 97: 3902–3909
38. Deininger MH, Weller M, Streffer J and Meyermann R (1999) Antiapoptotic Bcl-2 family protein expression increases with progression of oligodendroglioma. Cancer 86: 1832–1839
39. Ranger AM, Malynn BA and Korsmeyer SJ (2001) Mouse models of cell death. Nat. Genet. 28: 113–118
40. Brunet A and Datta SR (2001) Greenberg ME transcription-dependent and -independent control of neuronal survival by the PI3K-Akt signaling pathway. Curr. Opin. Neurobiol. 11: 297–305
41. Henshall DC, Clark RS, Adelson PD, Chen M, Watkins SC and Simon RP (2000) Alterations in bcl-2 and caspase gene family protein expression in human temporal lobe epilepsy. Neurology 55: 250–257
42. Henshall DC, Bonislawski DP, Skradski SL, Lan JQ, Meller R and Simon RP (2001) Cleavage of bid may amplify caspase-8-induced neuronal death following focally evoked limbic seizures. Neurobiol. Dis. 8: 568–580
43. Puthier D, Bataille R and Amiot M (1999) IL-6 up-regulates mcl-1 in human myeloma cells through JAK/STAT rather than ras/MAP kinase pathway. Eur. J. Immunol. 29: 3945–3950
44. Puthier D, Thabard W, Rapp M, Etrillard M, Harousseau J, Bataille R and Amiot M (2001) Interferon alpha extends the survival of human myeloma cells through an upregulation of the Mcl-1 anti-apoptotic molecule. Br. J. Haematol. 112: 358–363
45. Jee SH, Shen SC, Chiu HC, Tsai WL and Kuo ML (2001) Overexpression of interleukin-6 in human basal cell carcinoma cell lines increases anti-apoptotic activity and tumorigenic potency. Oncogene 20: 198–208
46. Epling-Burnette PK, Zhong B, Bai F, Jiang K, Bailey RD, Garcia R, Jove R, Djeu JY, Loughran Jr TP and Wei S (2001) Cooperative regulation of Mcl-1 by Janus kinase/stat and phosphatidylinositol 3-kinase contribute to granulocyte-macrophage colony-stimulating factor-delayed apoptosis in human neutrophils. J. Immunol. 166: 7486–7495
47. Fukuchi Y, Kizaki M, Yamato K, Kawamura C, Umezawa A, Hata J, Nishihara T and Ikeda Y (2001) Mcl-1, an early-induction molecule, modulates activin A-induced apoptosis and differentiation of CML cells. Oncogene 20: 704–713
48. Schubert KM and Duronio V (2001) Distinct roles for extracellular-signal-regulated protein kinase (ERK) mitogen-activated protein kinases and phosphatidylinositol 3-kinase in the regulation of Mcl-1 synthesis. Biochem. J. 356: 473–480
49. Garrido YC, Sanabria ER, Funke MG, Cavalheiro EA and Naffah-Mazzacoratti MG (1998) Mitogen-activated protein kinase is increased in the limbic structures of the rat brain during the early stages of *status epilepticus*. Brain Res. Bull. 47: 223–229
50. De Simoni MG, Perego C, Ravizza T, Moneta D, Conti M, Marchesi F, De Luigi A, Garattini S and Vezzani A (2000) Inflammatory cytokines and related genes are induced in the rat hippocampus by limbic *Status epilepticus*. Eur. J. Neurosci. 12: 2623–2633
51. Justicia C, Gabriel C and Planas AM (2000) Activation of the JAK/STAT pathway following transient focal cerebral ischemia: signaling through Jak1 and Stat3 in astrocytes. Glia 30: 253–270
52. Liu H, Perlman H, Pagliari LJ and Pope RM (2001) Constitutively activated Akt-1 is vital for the survival of human monocyte-differentiated macrophages Role of Mcl-1, independent of nuclear factor (NF)-kappaB, Bad, or caspase activation. J. Exp. Med. 194: 113–126
53. Clark RS, Kochanek PM, Watkins SC, Chen M, Dixon CE, Seidberg NA, Melick J, Loeffert JE, Nathaniel PD, Jin KL and Graham SH (2000) Caspase-3 mediated neuronal death after traumatic brain injury in rats. J. Neurochem. 74: 740–753
54. Didier M, Bursztajn S, Adamec E, Passani L, Nixon RA, Coyle JT, Wei JY and Berman SA (1996) DNA strand breaks induced by sustained glutamate excitotoxicity in primary neuronal cultures. J. Neurosci. 16: 2238–2250
55. Liang P, Zhu W, Zhang X, Guoo Z, O'Connell RP, Averboukh L, Wang F and Pardee AB (1994) Differential display using one-base anchored oligo-dT primers. Nucleic Acids Res. 22: 5763–5764
56. Burgess DL, Biddlecome GH, McDonough SI, Diaz ME, Zilinski CA, Bean BP, Campbell KP and Noebels JL (1999) beta subunit reshuffling modifies N- and P/Q-type Ca2+ channel subunit compositions in lethargic mouse brain. Mol. Cell Neurosci. 13: 293–311